

**NASA Technical Memorandum 87571**

NASA-TM-87571 19850023837

**INFLUENCE OF THE RESIN ON  
INTERLAMINAR MIXED-MODE  
FRACTURE**

**W. S. JOHNSON and P. D. MANGALGIRI**

**JULY 1985**

LIBRARY COPY

AUG 21 1985

LANGLEY RESEARCH CENTER  
LIBRARY, NASA  
HAMPTON, VIRGINIA



National Aeronautics and  
Space Administration

Langley Research Center  
Hampton, Virginia 23665

3 1176 01316 1857

m

## SUMMARY

Both literature review data and new data on toughness behavior of seven matrix and adhesive systems in four types of tests were studied in order to assess the influence of the resin on interlaminar fracture. Mixed mode (i.e. various combinations of opening mode I,  $G_I$ , and shearing mode II,  $G_{II}$ ) fracture toughness data showed that the mixed mode relationship for failure appears to be linear in terms of  $G_I$  and  $G_{II}$ . The study further indicates that fracture of brittle resins is controlled by the  $G_I$  component, and that fracture of many tough resins is controlled by total strain-energy release rate,  $G_T$ . Regarding the relation of polymer structure and the mixed mode fracture: high mode I toughness requires resin dilatation; dilatation is low in unmodified epoxies at room temperature/dry conditions; dilatation is higher in plasticized epoxies, heated epoxies, and in modified epoxies; modification improves mode II toughness only slightly compared with mode I improvements. Analytical aspects of the cracked lap shear test specimen were explored. Geometric nonlinearity must be addressed in calculating the  $G_I/G_{II}$  ratio. The ratio varies with matrix modulus, which in turn varies with moisture and temperature.

## INTRODUCTION

Fracture mechanics technology is being applied extensively to composite materials and adhesively bonded joints, primarily to determine the matrix and adhesive material toughness so as to aid in material development, screening, selection, and design. Efforts to determine toughness make use of the fact that the delamination failure mode in polymer matrix composites is very similar to the debonding of an adhesive joint: both the delamination and debond are usually "captured" between two boundary plies in the case of delamination, or adherends in the case of debonding. This physical restraint, in the presence of a mixture of external loads, can result in a variety of loading modes at the delamination or debond tip. These modes may range from pure mode I (opening or peel) through various combinations of mode I and mode II (sliding or shear) to pure mode II loading. Mode III (tearing) may even be present. Considerable effort has been made to identify proper test specimens and testing techniques for measuring the in situ toughness of composite matrix materials and adhesives. In particular, the relative influence of the mode I and mode II components on fracture has been of interest.

The purpose of this paper is to compare in situ toughness behavior of seven matrix and adhesive systems (as listed in table I) in order to assess the influence of resin on interlaminar fracture. Both brittle and tough systems will be addressed. Particular emphasis will be placed on the mixed mode influence on fracture. Although most of the data have been taken from the literature, some new data will be presented. The observed behavior of the different systems will be related to their chemical structures. Some analytical considerations for assessing mixed mode ratios will be presented.

## EXPERIMENTS

There are currently four tests widely used to measure interlaminar fracture toughness in terms of strain-energy release rate,  $G$ . Each test's specimen type is shown in figure 1. Shown first is the double cantilever beam (DCB) specimen, used to determine pure mode I toughness. Second is the edge delamination tensile (EDT) test specimen, used to examine a variety of mixed mode conditions, ranging from  $5.7 > G_I/G_{II} > 0.4$ , depending on specimen lay-up and geometry. Third is the cracked lap shear (CLS) specimen, which is also used to test a variety of mixed mode conditions, ranging from  $0.6 > G_I/G_{II} > 0.2$ , again depending on the specimen geometry. Pure mode II toughness is found by using the fourth specimen type in the end-notched flexure (ENF) test. All of these tests, except the EDT, are also used to characterize adhesives in bonded joints. All of the specimens, except the EDT, are calibrated by means of the general relationship between strain-energy release rate  $G$  and specimen compliance  $C$

$$G = \frac{P^2}{2b} \frac{dC}{da} \quad (1)$$

where  $P$  is the load,  $b$  the width, and  $a$  the crack length [1].

Although data acquired from tests involving all four of the above specimen types will be presented and discussed, only the CLS specimens were used to generate new data for this paper.

### Double Cantilever Beam Specimen

The pure mode I DCB specimen has been well documented for testing adhesives [2-4] and for testing interlaminar toughness of composites [5]. Linear beam theory can be used to determine  $G$  if the crack length is sufficiently long compared to the specimen adherend thickness,  $h$ . The compliance is

commonly expressed as  $C = 8 a^3 / b E h^3$  for plane stress conditions, where  $E$  is the longitudinal modulus of the adherends. This expression is valid as long as modulus is taken as apparent modulus. Ashizawa [6] presents correction factors for the flexural modulus. By expressing the derivative  $dC/da$  in terms of  $C$  and substituting into Eq (1), an expression for strain-energy release rate becomes

$$G = \frac{3P^2 C}{2ba} \quad (2)$$

The  $dC/da$  term can be calculated directly from the load-displacement plots of the experimental data. This technique is explained in references 5 and 7.

#### Edge Delamination Tensile Test Specimen

The EDT specimen is used to determine the interlaminar fracture toughness of composites only. The EDT test specimen and procedures have been fully documented by O'Brien [8]. The total strain-energy release rate can be calculated by

$$G = \frac{\epsilon^2 t}{2} (E_{LAM} - E^*) \quad (3)$$

where  $\epsilon$  = strain at delamination onset,

$t$  = specimen thickness,

$E_{LAM}$  = stiffness of the undamaged laminate, and

$E^*$  = stiffness of the laminate completely delaminated along one or more interfaces.

The effect of the crack length is accounted for by the  $E$  terms; therefore the crack length does not appear in Eq (3). The  $G_I/G_{II}$  ratio must be calculated by finite element analysis of the specimen lay-up of interest [8].

### Cracked Lap Shear Specimen

The CLS specimen was first used by Brussat, Chiu, and Mostovoy [9] for testing adhesively bonded metallic joints. Mall, Johnson, and Everett [7,10] used the CLS specimen to study adhesively bonded composite joints. Wilkins [5] was the first to successfully use the CLS specimen to measure mixed mode interlaminar fracture toughness in composites. An estimate for the total strain-energy release rate for the CLS specimen is given by

$$G = \frac{P^2}{2b^2} \left[ \frac{1}{(Eh)_2} - \frac{1}{(Eh)_1} \right] \quad (4)$$

where the subscripts 1 and 2 refer to the sections indicated in figure 1.

The total  $G$  can also be found from the experimental compliance measurements and Eq (1).

In order to get an accurate measure of the  $G_I$  and  $G_{II}$  components, a geometric nonlinear finite element model must be used [11]. This is because the lack of symmetry in the CLS specimen causes out-of-plane displacements and rotations. (This will be further discussed under Finite Element Analysis of CLS Specimens.)

### End-Notched Flexure Specimen

The ENF specimen is used to determine mode II toughness and was introduced by Russell [12]. The specimen is essentially the same as the DCB specimen, except that it is loaded in three-point bending. This loading condition results in pure shear loading at the crack tip. The Teflon starter strip supposedly allows no significant friction to occur between crack flanks. Under the bending, the crack does not open; thus mode I loading does not occur. Simple beam theory was used [12] to obtain the expression

$$G = \frac{9P^2 a^2 C}{2b (2L^3 + 3a^3)} \quad (5)$$

where L is the distance between the center and outer loading pins.

#### FINITE ELEMENT ANALYSIS OF CLS SPECIMENS

The cracked lap shear specimens (used to generate new data for this paper) were analyzed with the finite element program GAMNAS [11] to determine the strain-energy release rate for given geometry, debond length, and applied load. This two-dimensional analysis accounts for the geometric nonlinearity associated with the large rotations in the unsymmetrical cracked lap shear specimen.

The finite element mesh consisted of about 1700 isoparametric 4-node elements and had about 3700 degrees of freedom. The strip of matrix material was modeled with four layers of elements. A multipoint constraint was applied to the loaded end of the model to prevent rotation (i.e., all of the axial displacements along the ends are equal to simulate actual grip loading of the specimen). Plane-strain conditions were assumed in the finite-element analysis. The strain-energy release rate was computed using a virtual crack-closure technique. The details of this procedure are given in reference 13.

#### INFLUENCE OF THE POLYMER STRUCTURE

In order for a polymer to have a high mode I toughness, the material must be able to dilatate (increase volume) under plane-strain tensile loading. This volume increase can be from elastic, nonlinear elastic, or inelastic expansion. Mechanisms such as chain extension, crazing, void formation, and plasticity can contribute to the volume expansion. Those polymeric materials that are highly rigid due to a high degree of crosslinking (such as unmodified epoxies) are not normally able to exhibit much ability to dilatate.



Therefore, they will have a rather low mode I toughness. Figure 2 offers a schematic of resin stress-strain behavior and the stress concentrations at the crack tip in two resin systems, one tough and one brittle. Assuming that the resin at the crack tip is in a state of plane strain, the nonlinear stress-strain curve shown for the tough material can occur only if the material's volume increases. Notice that the shaded area under the two stress-strain curves is representative of the energy required for failure (i.e., the toughness). As can be seen in the figure, the plastic deformation (which must be accompanied by a volume expansion) requires considerable energy. Further, one should notice that the stress concentration at the crack tip is lower for those materials that exhibit plastic deformation, thus spreading the load over a larger area.

On the other hand, the polymer need not dilatate under the shearing deformation of mode II loading. Therefore, a highly crosslinked epoxy may have a much higher mode II toughness than mode I toughness. Specimens with a high percentage of mode II (shear) present have hackles on their fracture surfaces [14]. Pure shear stress can be resolved into a combination of tensile and compressive stresses. A simple Mohr's circles analysis will show that for pure shear stress the maximum tensile stress acts on a 45° plane. As a peel stress is added to the shear stress, the angle decreases. The maximum normal stress is expressed as

$$\sigma_{\max} = \frac{\sigma_1 + \sigma_2}{2} + \sqrt{\left(\frac{\sigma_1 - \sigma_2}{2}\right)^2 + \tau_{12}^2} \quad (6)$$

The maximum principal stress will act on a plane at  $\theta$  degrees to the adherend surface where

$$\tan 2\theta = \frac{\tau_{12}}{(\sigma_1 - \sigma_2)/2} \quad (7)$$

Therefore, when only shear stresses are present  $\theta = 45^\circ$ . When only peel stresses ( $\sigma_1$ ) are present  $\theta = 0^\circ$ . Pure mode II loading will result in the sharpest hackles. As the percent of mode I (peel) component increases, the hackles become less obvious, reflecting the fact that the angle of maximum tensile stress is decreasing toward  $0^\circ$ . The matrix material would be expected to fracture in a plane nearly perpendicular to the maximum tensile stress.

Both moisture and heat may increase the ability of polymers to dilatate, thus increasing the mode I toughness, but probably causing little improvement in the mode II toughness. Moisture may infuse into the polymer, separating the polymer molecules, thus reducing their secondary bond attraction, thereby making it easier for the molecules to move past each other. Moisture may also increase the critical strain levels. This process is a form of plasticization. Heat creates a similar effect. The higher temperature, especially approaching the glass transition temperature, causes the material to expand, thus creating more free volume. This increase in free volume allows the molecules to move past each other more easily.

Rubber toughened epoxies have a propensity to dilatate by the stretching of the rubber particles and the formation of internal voids. Thus rubber toughened epoxies such as FM-300 and EC 3445 could have  $G_{IC}$  values as high as the  $G_{IIC}$  values. Bascom, Cottingham and Timmons [4] suggest that the rubber modified epoxies exhibit large increases in toughness with relatively little loss in high tensile strength, modulus, or thermal mechanical resistance of the epoxy matrix resin. They further suggest that the rubber particles allow a much larger volume for plastic deformation at the crack tip than allowed by the unmodified epoxy resins. This deformation involves a more or

less symmetrical dilatation of the rubber particles accompanied by plastic flow of the epoxy. The problem with the highly rubber modified epoxies and the linear systems is that they become so ductile in the presence of heat and moisture that they usually cannot function as a structural material.

Dilatation can be seen in polysulfones, linear systems that are essentially masses of polymer chains that are intertwined but not physically linked together as epoxies are. These linear systems are more ductile and can dilatate more than the unmodified epoxies. (Polysulfone data are not presented in this paper.)

Other modifications can also contribute to improving the material toughness; one example is chain-extended epoxies such as the Hx205 resin. Although the material is still crosslinked, the extended chains can behave somewhat like linear systems, thus improving the  $G_I$  toughness. At the same time, they are expected to display more viscoelastic behavior and to be more sensitive to temperature and moisture conditions.

Crystalline resins such as PEEK have a toughening mechanism consisting of chains unfolding. They also have a strengthening mechanism consisting of the crystals slipping in order to achieve a structure oriented in the direction of the stress.

## RESULTS AND DISCUSSION

### Toughness Data

This section will present mixed mode interlaminar fracture toughness results for brittle systems (T300/5208 and AS1/3501-6 composites) and tougher systems (FM-300 and EC 3445 adhesives, and Hx205, F-185, and PEEK matrix composites). Figures displaying toughness data will be labeled as to specimen type,  $G_I/G_{II}$  ratio, and source reference. Where no reference is given, the data were generated by the authors.

## Brittle Systems

T300/5208 - The interlaminar fracture envelope for T300/5208 composites is shown in figure 3. The  $G_I$  component at fracture is plotted against the  $G_{II}$  component at fracture. The sum of the  $G_I$  and  $G_{II}$  components is the total strain-energy release rate  $G_T$ . The value of the critical mode I strain-energy release rate ( $G_{IC}$ ) is approximately one-tenth of the critical mode II strain-energy release rate ( $G_{IIC}$ ). The mixed mode fractures appear to be controlled by the  $G_I$  component. This is a good example of an unmodified epoxy with limited dilatational ability having a much lower  $G_{IC}$  than  $G_{IIC}$ . The scatter bands represent the maximum, minimum, and average values of the data. Notice that the source is given for each specimen type. The CLS data were generated for this paper and are presented in table II.

AS1/3501-6 - Another rather brittle unmodified epoxy system is 3501-6. The AS1/3501-6 system has been extensively studied by Russell [12], Russell and Street [17], Wilkins [5], Law and Wilkins [18], and Jurf and Pipes [19] to determine interlaminar fracture toughness. Figure 4 shows some of Russell and Street's [17] results using the DCB, CLS, and ENF specimens. The data spread is plus or minus one standard deviation from the mean of their results. Their data indicate that  $G_{IIC}$  is about 3.5 times higher than  $G_{IC}$ . This  $G_{IC}$  value is about 50 percent higher than the  $G_{IC}$  for the 5208 matrix.

Law and Wilkins [18] tested DCB specimens and three geometries of the CLS specimen to assess the effects of heat and moisture on mixed mode fracture. The DCB data were 100 percent mode I. The CLS specimens had  $G_I/G_{II}$  ratios of 0.20, 0.42, and 0.59. The specimens with 0.20 and 0.42 ratios were tested wet and dry at 93°C and 22°C, as were the DCB specimens. These data are plotted in figure 5. The 22°C/dry data are almost horizontal, indicating a  $G_I$ -dominated fracture mode. The  $G_I$  is very low compared to the  $G_{II}$

components. However, as heat is applied (93°C/dry) the  $G_I$  increases while the  $G_{II}$  components remain about the same. When moisture is introduced (22°C/wet), the  $G_I$  increases and the  $G_{II}$  components appear to decrease. When both heat and moisture are introduced (93°C/wet),  $G_I$  increases markedly, while the  $G_{II}$  appears to be substantially reduced.

These results by Law and Wilkins [18] are somewhat clouded by the fact that the DCB specimens showed considerable fiber bridging, particularly at the higher temperature and wet conditions. Therefore the DCB values are probably artificially higher than those of the matrix material. The CLS specimens did not have this problem. In fact, Russell and Street [17] indicated that the DCB specimen toughness did not increase with temperature when only the initial crack extension was used to calculate  $G_I$ , thus avoiding the fiber bridging problem encountered at longer crack lengths. Hunston and Bascom also report little increase in toughness with increasing temperature for unmodified epoxies [20]. This is perplexing because Russell and Street also showed that the neat specimens of 3501-6 showed improvements in toughness with increasing temperature. Perhaps the fact that these "initial" crack extensions were from the Teflon starter caused the toughness to be insensitive to the environmental effects. The Teflon starter may be rather blunt compared to a natural delamination, thereby causing the toughness to be high.

#### Tough Systems

FM-300 - FM-300 is a nitride rubber-modified, epoxy-structured adhesive widely used in the aerospace industry. It is a mat reinforced film adhesive cured at 176°C; the resulting bondline is 0.25 mm thick. Mall and Johnson [7] determined the mode I and mixed mode fracture toughness using DCB and two different geometries of the CLS specimen. These CLS specimens had  $G_I/G_{II}$  ratios of 0.33 and 0.38. The  $G_{Ic}$  toughness, shown in figure 6, is 7 to 10

times greater than previously found for the brittle systems (i.e., 5208 and 3501-6) at room temperature and dry. The apparent  $G_{IIc}$  toughness (extrapolated from the CLS and DCB data) is a little over twice that of the 3501-6 and about equal to that of the 5208. The rubber toughening greatly improves the  $G_{Ic}$  but is less effective on the shearing mode  $G_{IIc}$ . Even though the DCB adherends were made of unidirectional T300/5208 composites, the data reported in figure 6 all show cohesive failures in the adhesive; there was, of course, no fiber bridging.

EC 3445 - EC 3445 is also a rubber-modified, epoxy-structured adhesive that is currently used in the aerospace industry. It has 121°C cure temperature. The resin is a one-part paste. Glass beads are used to maintain a bondline thickness of 0.10 mm.

Mall and Johnson [7] determined the mode I and mixed mode fracture toughness for the EC 3445 as they did for FM-300. Figure 6 shows results for both. As previously discussed for the FM-300, the  $G_{Ic}$  and apparent  $G_{IIc}$  are practically the same. Two geometries of the CLS specimen were also tested, resulting in  $G_I/G_{II}$  ratios of 0.25 and 0.31.

Hx205 - The Hx205 base resin is a standard bisphenol A diglycidyle ether modified with an epoxy novolac and chain extended with additional bisphenols. The Hx205 was chosen for study because it has high toughness. As such, it is an appropriate material to use in evaluating methods for testing interlaminar toughness and mixed mode fracture. However, it is not used for structural composite matrices because of its low  $T_g$  (100°C) and poor hot-wet mechanical properties. Figure 7 presents the fracture envelope for Hx205 matrix composites tested in a laboratory environment. The data spread in figure 7 represents the maximum, minimum, and average values of the data for each specimen type. The CLS data for the Hx205 are given in table III.

F-185 - F-185 is a commercially available adhesive. It is essentially a rubber modified form of Hx205. Figure 8 shows the DCB data developed by Hunston [21] and the EDT data of O'Brien, Johnston, Morris, and Simonds [22]. The  $G_{IC}$  is much higher than the  $G_{IC}$  values of the other resin systems presented. The  $G_{IC}$  value is quite close to the apparent  $G_{IIc}$  value (extrapolating the data to the  $G_{II}$  axis). Apparently both rubber toughening and extending molecular chains individually contribute to the overall toughness of a material. The effect of extending molecular chains can be seen by the substantial increase in the chain-extended Hx205 system over the unmodified epoxies (3501-6 and 5208). F-185 shows a substantial improvement in toughness over Hx205 due to rubber toughening.

PEEK - The PEEK matrix material is a polyetheretherketone, a high temperature thermoplastic which has a semi-crystalline structure. (This resin is also designated as ICI VICTREX APC2.) Russell and Street [23] determined the interlaminar toughness of AS4/PEEK using the DCB and ENF specimens. Their values for the  $G_{IC}$  are  $1330 \pm 85 \text{ J/m}^2$  (mean  $\pm$  standard deviation). Using the ENF specimen they determined  $G_{IIc}$  to be  $1765 \pm 235 \text{ J/m}^2$ . The value of  $G_{IIc}$  is approximately 1.3 times  $G_{IC}$ .

#### Data Trends

Data for a variety of matrix and adhesive systems have been presented and discussed. Mixed mode fracture toughness for each system is shown in figure 9, which is in large part a plot of the mean data points from figures 3, 4, 6, 7, and 8. In general, the higher the  $G_{IC}$  value, the closer  $G_{IC}$  is to  $G_{IIc}$ . The brittle materials are much more sensitive to the  $G_I$  components than are the tougher materials. The tougher materials are almost equally sensitive to  $G_I$  and  $G_{II}$ .

### Static Failure Criteria

A failure criterion based on  $G$  has been expressed by several investigators [17,24] in the form of

$$\left[ \frac{G_I}{G_{Ic}} \right]^m + \left[ \frac{G_{II}}{G_{IIc}} \right]^n = 1 \quad (6)$$

As can be seen from the sampling of resin toughness data shown in figure 9, a straight line relationship does a good job of fitting the given data for each material. This simplifies Eq (6) to

$$\frac{G_I}{G_{Ic}} + \frac{G_{II}}{G_{IIc}} = 1 \quad (7)$$

For the tougher resin materials where  $G_{Ic}$  is very nearly equal to  $G_{IIc}$ , we can assume

$$G_{Ic} = G_{IIc} = G_c \quad (8)$$

Substituting Eq (8) into Eq (7) results in

$$G_I + G_{II} = G_T = G_c \quad (9)$$

where  $G_c$  is the critical total strain-energy release rate. The total strain-energy release rate,  $G_T$ , is much simpler to calculate than individual components  $G_I$  and  $G_{II}$  [7,10]. Simple strength of materials approaches often give adequate estimates of  $G_T$  whereas they do poorly predicting  $G_I$  and  $G_{II}$  components. Therefore, even if  $G_{Ic}$  does not exactly equal  $G_{IIc}$ , the  $G_T$  concept for design purposes may be economically justifiable. Thus Eq (9) is a reasonable static failure criterion for many tough resin systems while Eq (7) may be appropriate for brittle materials.



### Related Data

Jordan and Bradley [14] have developed interlaminar toughness data on AS4/3502 and T3T145/F155 composites using symmetrically and asymmetrically loaded split laminates. They found for AS4/3502 material  $G_{IC} = 190 \text{ J/m}^2$  and  $G_{IIC} = 570 \text{ J/m}^2$ , and for the T3T145/F155 material  $G_{IC} = 431 \text{ J/m}^2$  and  $G_{IIC} = 1800 \text{ J/m}^2$ . As in other cases of somewhat low  $G_{IC}$  values, the ratio  $G_{IC}/G_{IIC}$  is quite low.

### Effect of Environment

Further, figure 5 gives evidence that for a given resin (3501-6 in this case) the  $G_{IC}$  of the system may increase while the  $G_{IIC}$  may remain the same or even decrease under different environmental conditions. Whereas a resin may be  $G_I$  sensitive under the cold/dry condition,  $G_{IC}$  may approach  $G_{IIC}$  and make the system appear to be  $G_T$  sensitive in conditions of increased temperature and moisture.

### Analytical Considerations

This section will present several analyses of the CLS specimens using the finite element program GAMNAS as explained earlier. The influence of geometric nonlinear behavior and the influence of changing matrix material modulus due to heat and moisture on the  $G_I/G_{II}$  ratio are evaluated.

Geometric Nonlinear Effects - Law and Wilkins [18] used a geometric nonlinear finite elements program to calculate the  $G_I/G_{II}$  ratios of the CLS data shown in figure 5. Russell and Street [17] used the average value of a strength of materials approach suggested by Brussat, Chiu, and Mostovoy [9] and a linear finite element program to calculate the  $G_I/G_{II}$  ratio for the CLS data shown in figure 4.

Figure 10 shows our results using the geometric nonlinear analysis. The results are for a 3-ply to 3-ply AS1/3501-6 CLS specimen. The  $G_I/G_{II}$  ratio is plotted versus the total strain-energy release rate,  $G_T$ . The  $G_I/G_{II}$  ratios from linear finite element analysis and the strength of materials formulation are shown for comparison. Notice that only the geometric nonlinear finite element analysis indicated an increase in  $G_I/G_{II}$  ratio with  $G_T$ . It is clear that nonlinear analysis should be used for CLS specimens, as explained by Wilkins [5] and Dattaguru, Everett, Whitcomb, and Johnson [11]. The tougher matrix requires higher load for fracture, thus resulting in more nonlinear response. Therefore the tougher the matrix, the greater the error in using a linear finite element program or the strength of materials approach. Russell and Street [17] used a  $G_I/G_{II}$  ratio of 0.25 for their CLS specimen; according to figure 10 the value is closer to 0.42, the value used by Law and Wilkins [18]. It should be added that the strength of materials solution in this case is close to the linear finite element analysis only because the adherends are of equal thickness. If the adherends were of different thickness there would not be such a close agreement [11].

It should also be clear that if the toughness is influenced by heat and moisture, the  $G_I/G_{II}$  ratio is also influenced. For example, if a hot/wet condition causes the matrix toughness to increase, then more load will be required to achieve the higher  $G_T$ . From figure 10 it is quite clear that the  $G_I/G_{II}$  ratio is sensitive to variations in  $G_T$  in the proximity of the 3501-6 toughness.

Matrix Modulus Effects - Augl [25] has shown that the shear and Young's modulus of 3501-6 can decrease almost an order of magnitude from room temperature/dry to 121°C/wet. The shear modulus decreases by 32 percent at 60°C/wet. We decided to investigate what effect matrix modulus changes would have on

calculated  $G_I/G_{II}$  ratios. Using DCB specimens with BP907 adhesive, Chai [26] has determined that an adhesive joint bond thickness of 0.064 mm. or less would give the same toughness as an interlaminar fracture toughness test in a composite. Therefore, we modeled a thin strip of AS1/3501-6 matrix materials using a finite element method as one would model an adhesive joint [10]. The matrix strip was evaluated for thicknesses of 0.025 mm. and 0.0125 mm. Only the matrix material in the adhesive layer was changed to simulate temperature and moisture conditions; the adherend properties were not changed.

Figure 11 shows the results using the CLS-63 (i.e., 3 plies to 3 plies) specimen geometry and adherend properties that Law and Wilkins [16] tested. The  $G_I/G_{II}$  ratios were calculated for several load levels and for three different values of Young's moduli for the matrix: 4.28 GPa (21°C/0% RH); 2.39 GPa (100°C/80% RH); and 0.56 GPa (150°C/80% RH) [25].

The calculated results shown in figure 11 indicate that little change in  $G_I/G_{II}$  ratio occurs at temperatures below 100°C. The decrease of the RT/dry matrix modulus by approximately one-half decreased the  $G_I/G_{II}$  ratio by at most 11 percent. The  $G_T$  value remains constant over this range. As the matrix modulus decreases further, the  $G_I/G_{II}$  ratio changes become more pronounced, particularly at the higher loads. The  $G_I/G_{II}$  ratio changes are primarily attributed to the geometric nonlinear effects, as previously discussed. This may be readily seen by the fact that the  $G_I/G_{II}$  ratio changed very little at the lower load levels. The authors have no explanation for the crossover point in the  $G_I/G_{II}$  behavior except that perhaps the shear modulus has become so low that shear stresses and deformations dominate the specimen's bondline.

This section showed that decreases in matrix modulus due to moderate heat (below 100°C) and moisture do not affect  $G_I/G_{II}$  ratio calculations to a

significant degree. However, this study did not cover changing adherend properties, nor did it consider material nonlinear effects. Furthermore, it should be noted that 3501-6 is an unmodified, highly crosslinked epoxy system. One would expect its modulus to be less affected by heat and moisture than those of many modified or rubber toughened epoxies, such as Hx205 or FM-300. In these tougher materials the decrease in modulus may be very significant and should be accounted for in the determination of  $G_I/G_{II}$ .

#### CONCLUDING REMARKS

The literature has been reviewed and new data developed for assessing the influence of resin on interlaminar fracture. Data from four specimen types have been studied: Double cantilever beam for pure mode I, the edge delamination tensile test for mixed mode I and II, the cracked lap shear for mixed mode I and II, and the end-notched flexure for pure mode II. Mixed mode fracture data for seven resins were examined: 5208, 3501-6, FM-300, EC 3445, Hx205, F-185, and PEEK. From the presented mixed mode fracture data the following was evident:

- o The mixed mode relationship for failure appears to be linear in terms of  $G_I$  and  $G_{II}$ .
- o Fracture of brittle resins (low  $G_{IC}$ ) is controlled by the  $G_I$  component.
- o Fracture of many tough resins (high  $G_{IC}$  where  $G_{IC} \approx G_{IIc}$ ) is controlled by the total strain-energy release rate  $G_T$ . Because of the simplicity of calculation,  $G_T$  is a good failure criterion for design.

A short explanation of how the polymer structure directly relates to the mixed mode was given. The following were hypothesized and supported by the data:

- o Volume expansion (dilatation) must occur if high opening mode toughness is to be achieved.
- o Unmodified epoxies have limited ability to dilatate at room temperature/dry conditions, resulting in low values of  $G_{IC}$ .
- o Plasticized epoxies and those at higher temperatures have more free volume; therefore their ability to dilatate increases, resulting in higher values of  $G_{IC}$ .
- o Modified epoxies (rubber toughening/extended chains) have increased ability to dilatate; therefore they have higher  $G_{IC}$  values.
- o Shear deformation does not require volume dilatation; therefore there is only a limited amount of  $G_{IIC}$  improvement by modification.

Several analytical aspects of the cracked lap shear specimen were

explored:

- o Significant errors in the calculation of  $G_I/G_{II}$  ratios could result if geometric nonlinear aspects of the problem were not addressed. The tougher the matrix, the larger the error.
- o The  $G_I/G_{II}$  ratio was also found to vary with matrix modulus, which in turn varied with moisture and temperature. For 3501-6 resin, this variation was not large below 100°C.

## REFERENCE

- [1] Irwin, G. R., "Fracture Mechanics", Structural Mechanics, Goodier and Hoff, Ed., Pergamon Press, New York, 1960, p. 557.
- [2] Ripling, E. J., Mostovoy, S., and Patrick, R. L., "Application of Fracture Mechanics to Adhesive Joints", ASTM STP 360, American Society for Testing and Materials, 1963.
- [3] Mostovoy, S., and Ripling, E. J., "Fracture Toughness of an Epoxy System," Journal of Applied Polymer Science, Vol. 10, 1966, pp. 1351-1371.
- [4] Bascom, W. D., Cottingham, R. L., and Timmons, C. O., "Fracture Reliability of Structural Adhesives", Journal of Applied Polymer Science: Applied Polymer Symposium 32, 1977, pp. 165-188.
- [5] Wilkins, D. J., "A Comparison of the Delamination and Environmental Resistance of a Graphite-Epoxy and a Graphite-Bismaleimide", NAV-GD-0037, Naval Air Systems Command, September 1981. (DTIC ADA-112474)
- [6] Ashizawa, M., "Improving Damage Tolerance of Laminated Composites Through the Use of New Tough Resins", Proceedings of the 6th Conference on Fibrous Composites in Structural Design, AMMRC MS 83-2, Army Materials and Mechanics Research Center, Watertown, MA, Nov. 1983, pp. IV-21.
- [7] Mall, S., and Johnson, W. S., "Characterization of Mode I and Mixed Mode Failure of Adhesive Bonds Between Composite Adherends", NASA TM 86355, Washington, D.C., February 1985 (also to appear in Composite Materials: Testing and Design (Seventh Conference) ASTM STP, 1985)

- [8] O'Brien, T. K., "Characterization of Delamination Onset and Growth in a Composite Laminate", Damage in Composite Materials, ASTM STP 775, K. L. Reifsnider, Ed., American Society for Testing and Materials, 1982, pp. 140-167.
- [9] Brussat, T. R., Chiu, S. T., and Mostovoy, S., "Fracture Mechanics for Structural Adhesive Bonds", AFML-TR-77-163, Air Force Materials Laboratory, Ohio, 1977.
- [10] Mall, S., Johnson, W. S., and Everett, R. A., Jr., "Cyclic Debonding of Adhesively Bonded Composites", Adhesive Joints, K. L. Mittle, Ed., Plenum Press, New York, 1984, pp. 639-658.
- [11] Dattaguru, B., Everett, R. A., Jr., Whitcomb, J. D., and Johnson, W. S., "Geometrically Non-Linear Analysis of Adhesively Bonded Joints", Journal of Engineering Materials and Technology, January 1984, Vol. 106, pp. 59-65.
- [12] Russell, A. J., "On the Measurement of Mode II Interlaminar Fracture Energies", DREP Materials Report 82-0, Defense Research Establishment Pacific, Victoria, BC, 1982.
- [13] Rybicki, E. F., and Kanninen, M. F., "A Finite Element Calculation of Stress Intensity Factors by a Modified Crack Closure Integral", Engineering Fracture Mechanics, Vol. 9, No. 4, 1977, pp. 931-939.
- [14] Jordan, W. M., and Bradley, W. L., "Micromechanisms of Fracture in Toughened Graphite-Epoxy Lamintes", Toughened Composites, ASTM STP, N. J. Johnston, Ed., 1987.
- [15] O'Brien, T. K., "Mixed Mode Strain-Energy-Release Rate Effects on Edge Delamination of Composites", Effects of Defects in Composite Materials, ASTM STP 836, Am. Soc. of Testing and Materials, 1984, pp. 125-142.

- [16] Murri, G. B., and O'Brien, T. K., "Interlaminar  $G_{IIC}$  Evaluation of Toughened-Resin Matrix Composites using the End-Notched Flexure Test", Proceeding of 26<sup>th</sup> AIAA/ASME/ASCE/AHS Structural Dynamics and Materials Conf. Part I, Orlando, Florida, April 15-17, 1985, pp. 197-202.
- [17] Russell, A. J., and Street, K. N., "Moisture and Temperature Effects on the Mixed-Mode Delamination Fracture of Unidirectional Graphite/Epoxy", Delamination and Debonding of Materials, ASTM STP 876, W. S. Johnson, Ed., American Society of Testing and Materials, 1985.
- [18] Law, G. E., and Wilkins, D. J., Delamination Failure Criteria for Composite Structures, NAV-GD-0053, Naval Air Systems Command, Washington, D.C., 15 May 1984.
- [19] Jurf, R. A., and Pipes, R. B., "Interlaminar Fracture of Composite Materials", Journal of Composite Materials, Vol. 16, No. 5, Sept. 1982, pp. 386-394.
- [20] Hunston, D. L., and Bascom, W. D., "Effects of Lay-Up, Temperature, and Loading Rate in Double Cantilever Beam Tests of Interlaminar Crack Growth", Composite Technology Review, Vol. 5, Winter 1983, pp. 118-119.
- [21] Hunston, D. L., "Composite Interlaminar Fracture: Effect of Matrix Fracture Energy", Composite Technology Review, Vol. 6, No. 4, Winter 1984, pp. 176-180.
- [22] O'Brien, T. K., Johnston, N. J., Morris, D. H., and Simonds, R. A., "Determination of Interlaminar Fracture Toughness and Fracture Mode Dependence of Composites using the Edge Delamination Test," Proceedings of the International Conference on Testing, Evaluation, and Quality Control of Composites, September 13-14, 1983, University of Surrey, Guildford, England, T. Feest, Ed., Butterworths, London, 1983, pp. 223-232.



- [23] Russell, A. J., and Street, K. N., "The Effect of Matrix Toughness on Delamination: Static and Fatigue Fracture Under Mode II Shear Loading of Graphite Fiber Composites", Toughened Composites, ASTM STP, N. J. Johnston, Ed., 1987.
- [24] Ramkumar, R. L., and Whitcomb, J. D., "Characterization of Mode I and Mixed Mode Delamination Growth in T300/5208 Graphite/Epoxy", Delamination and Debonding of Materials, ASTM STP 876, W. S. Johnson, Ed., Am. Soc. for Testing and Materials, 1985.
- [25] Augl, J. M., "Moisture Effects on the Mechanical Properties of Hercules 3501-6 Epoxy Resin", NSWC TR 79-41, Naval Surface Weapons Center, Silver Springs, MD, 30 March 1979.
- [26] Chai, H., "On the Bond Thickness Effect in Adhesive Joints and Its Significance to Composites Mode I Interlaminar Fracture," Composite Materials: Testing and Design (Seventh Conference), ASTM STP, 1985.

Table I: Resin systems

Resins**	Polymer structure	Supplier**
5208	Epoxy - unmodified	Narmco
3501-6	Epoxy - unmodified	Hercules
FM-300*	Epoxy - chain extended	Hexcel
EC 3445*	Epoxy - chain extended/ rubber modified	Hexcel
Hx205	Epoxy - rubber modified	3-M
F-185*	Epoxy - rubber modified	American Cyanamid
PEEK	Semi-crystalline	Imperial Chemical Industries

\*Commercial adhesive.

\*\*Use of trade or manufacturer names does not constitute an official endorsement, expressed or implied, by the National Aeronautics and Space Administration.

Table II: Cracked lap shear fracture toughness tests data for T300/5208  
(3 plies to 3 plies)

Specimen no.	Delamination length	Critical load	Strain-energy release rate		
	a	$P_C$	Mode I $G_I$	Mode II $G_{II}$	Total $G_C$
	mm	kN	J/m <sup>2</sup>	J/m <sup>2</sup>	J/m <sup>2</sup>
1	36.8	5.40	52.6	126.4	178
	80.3	5.51	53.6	131.4	185
	101.6	5.27	49.0	120.0	169
	119.1	5.68	53.1	129.9	183
2	35.6	5.84	76.2	181.8	256
	53.3	5.36	62.1	151.9	214
	88.9	5.40	63.8	156.2	220
	110.5	5.45	64.7	158.3	223
	130.8	5.34	62.1	151.9	214
	143.5	5.49	65.8	161.2	227
3	35.6	5.74	71.9	176.1	248
	62.2	5.51	66.1	161.9	228
	68.6	5.57	67.9	166.1	234
	78.1	5.67	70.2	171.8	242
	116.8	5.41	64.1	156.9	221
	128.9	5.54	67.0	164.0	231
	166.4	5.31	61.5	150.5	212
4	34.3	5.79	72.2	176.8	249
	85.6	5.52	65.8	161.2	227
	104.6	5.47	64.7	158.3	223
	128.0	5.56	66.7	163.3	230

Table III: Cracked lap shear fracture toughness tests data for T6C/Hx205  
(6 plies to 6 plies)

Specimen no.	Delamination length	Critical load	Strain-energy release rate		
	a	P <sub>c</sub>	Mode I G <sub>I</sub>	Mode II G <sub>II</sub>	Total G <sub>c</sub>
	mm	kN	J/m <sup>2</sup>	J/m <sup>2</sup>	J/m <sup>2</sup>
1	29.7	17.61	376	672	1048
	38.4	19.26	450	803	1253
	68.8	19.02	439	782	1221
	96.0	19.17	446	795	1241
	114.0	19.53	463	825	1288
2	28.7	20.37	490	873	1363
	57.2	19.75	460	821	1281
	82.3	19.79	462	826	1286
	101.1	19.99	472	841	1313
3	27.2	20.14	335	599	934
	39.1	20.46	346	617	963
	51.8	20.18	337	600	937
	70.9	20.08	333	595	928
4	26.9	19.70	462	825	1287
	35.8	20.08	480	857	1337
	53.6	20.17	485	864	1349
	114.8	19.77	466	830	1296
	144.5	19.37	447	797	1244
	166.1	19.55	455	812	1267

- Double cantilever beam flexure test (tension)

- Edge delamination tensile test (mixed tension/shear)

- Cracked lap shear test (mixed tension/shear)

- End-notched flexure test (shear)

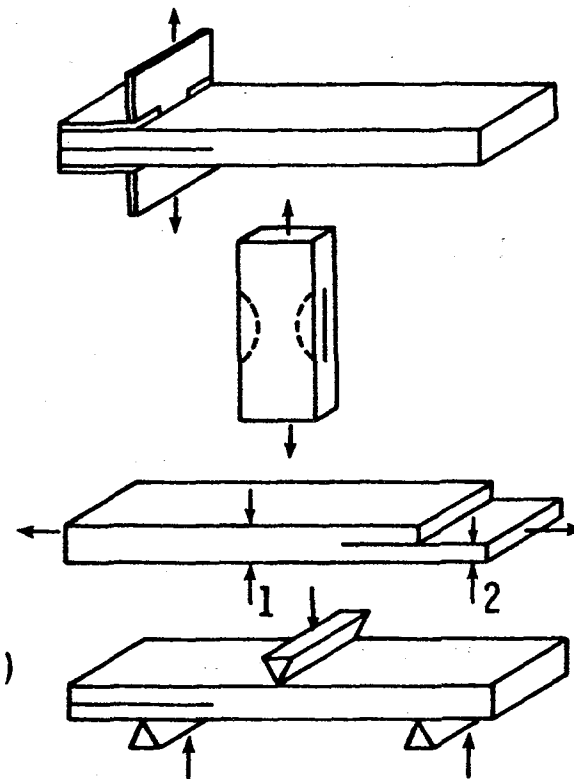


Figure 1 - Four specimen types used for determination of interlaminar fracture toughness.

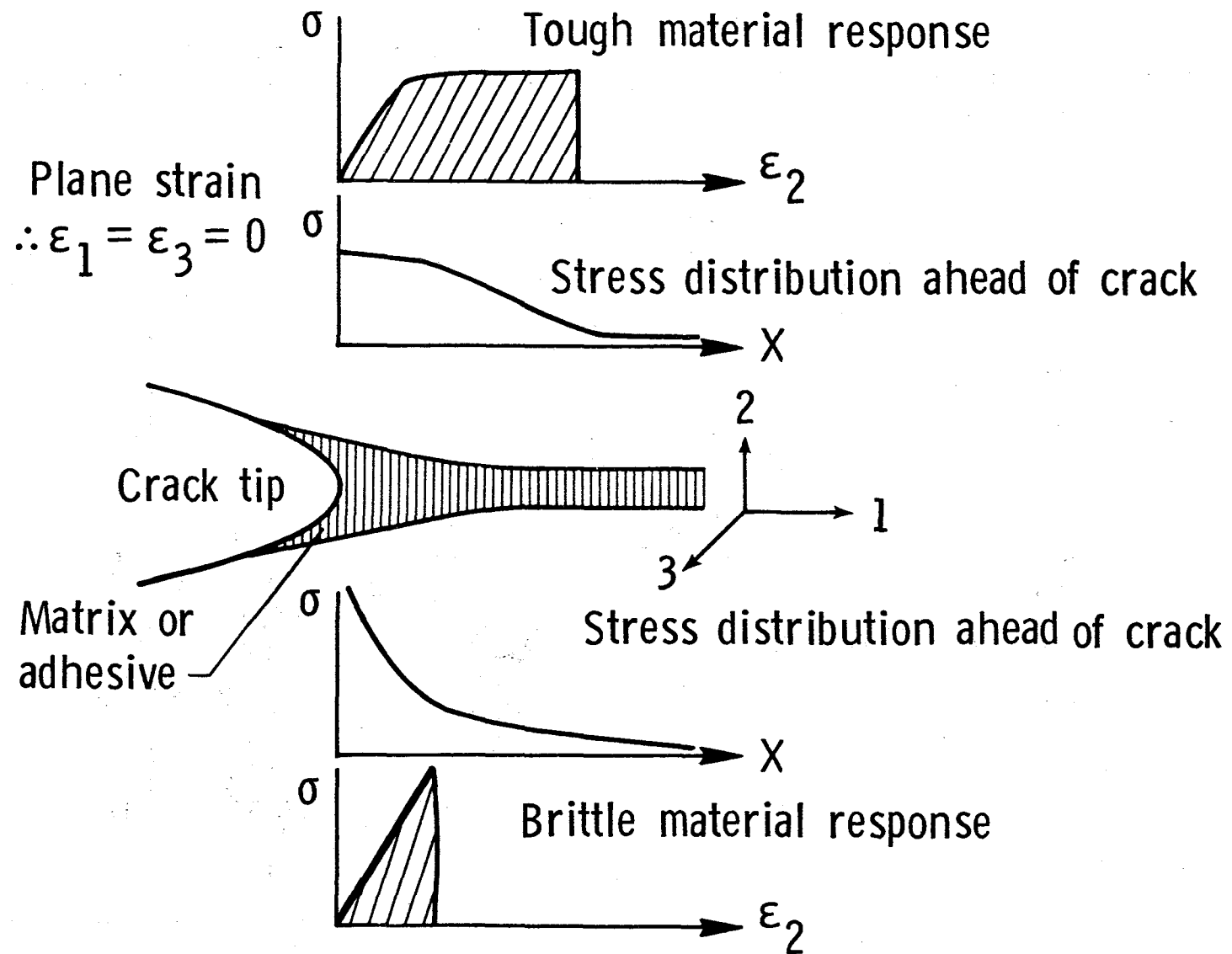


Figure 2 - Schematic of resin stress-strain behavior and stress distribution at the crack tip.

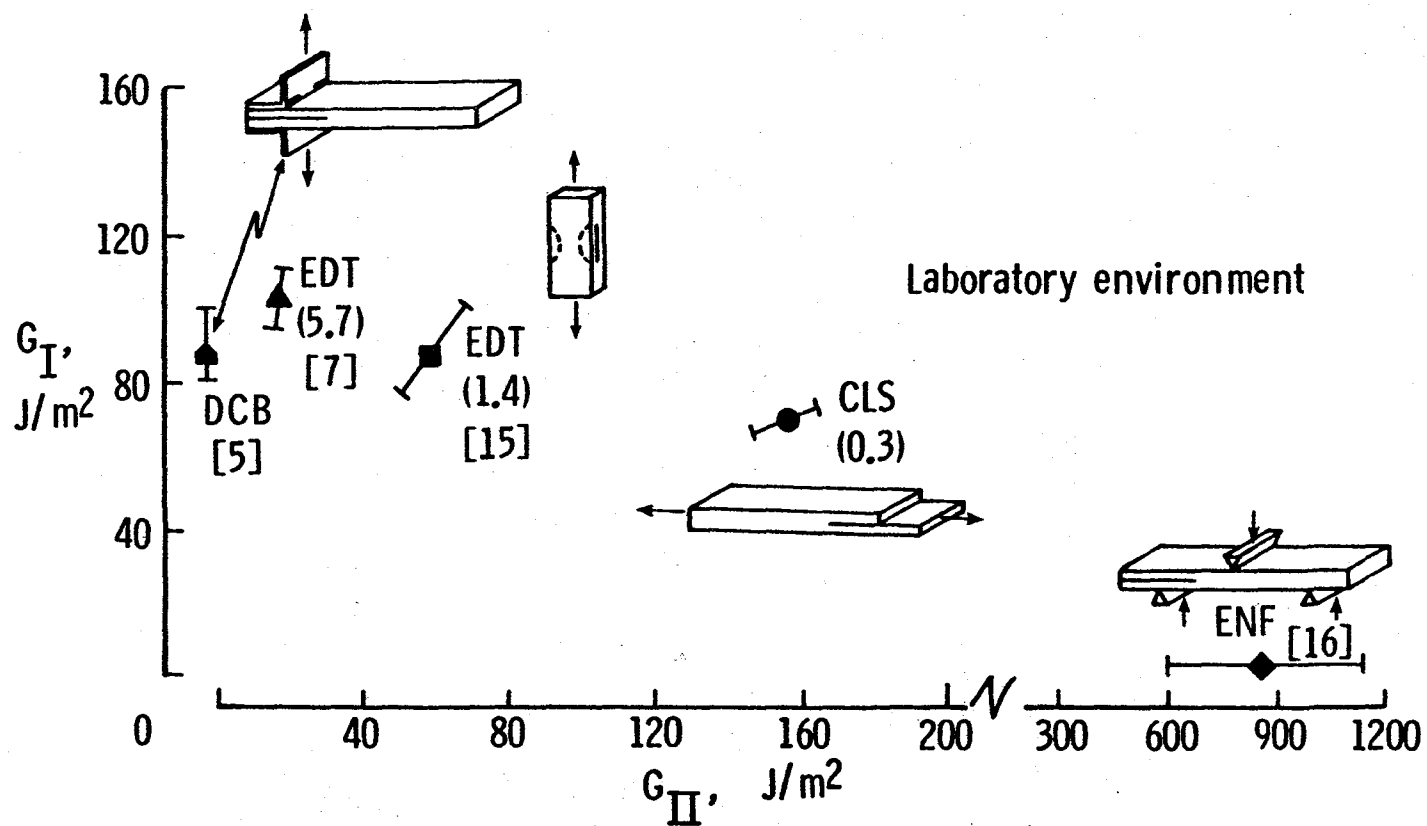


Figure 3 - Interlaminar fracture toughness of T300/5208 composites. The data spread is the maximum and minimum values.

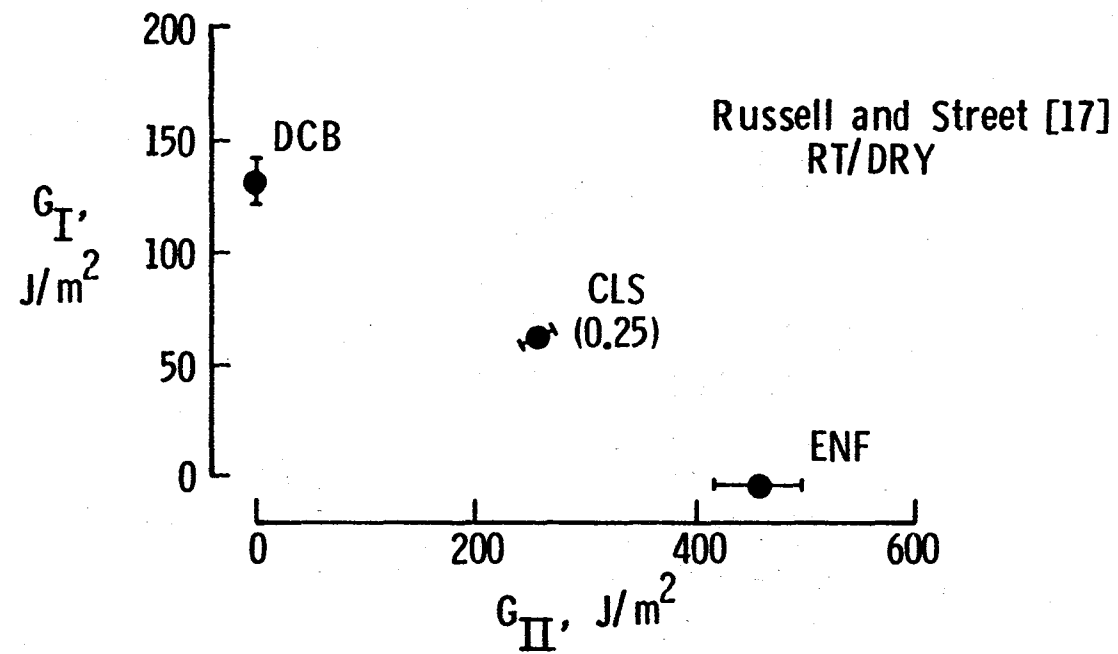


Figure 4 - Interlaminar fracture toughness of AS1/3501-6 composites. The data spread is one standard deviation from the mean.



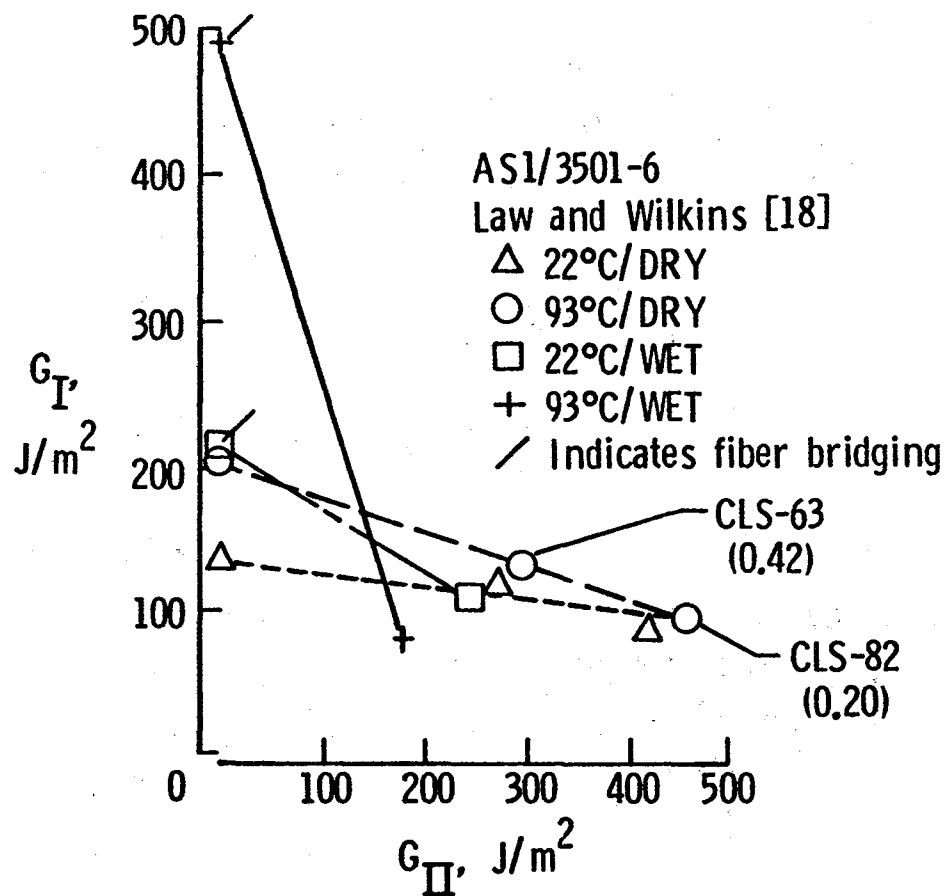


Figure 5 - Interlaminar fracture toughness of AS1/3501-6 composites under various environmental conditions.

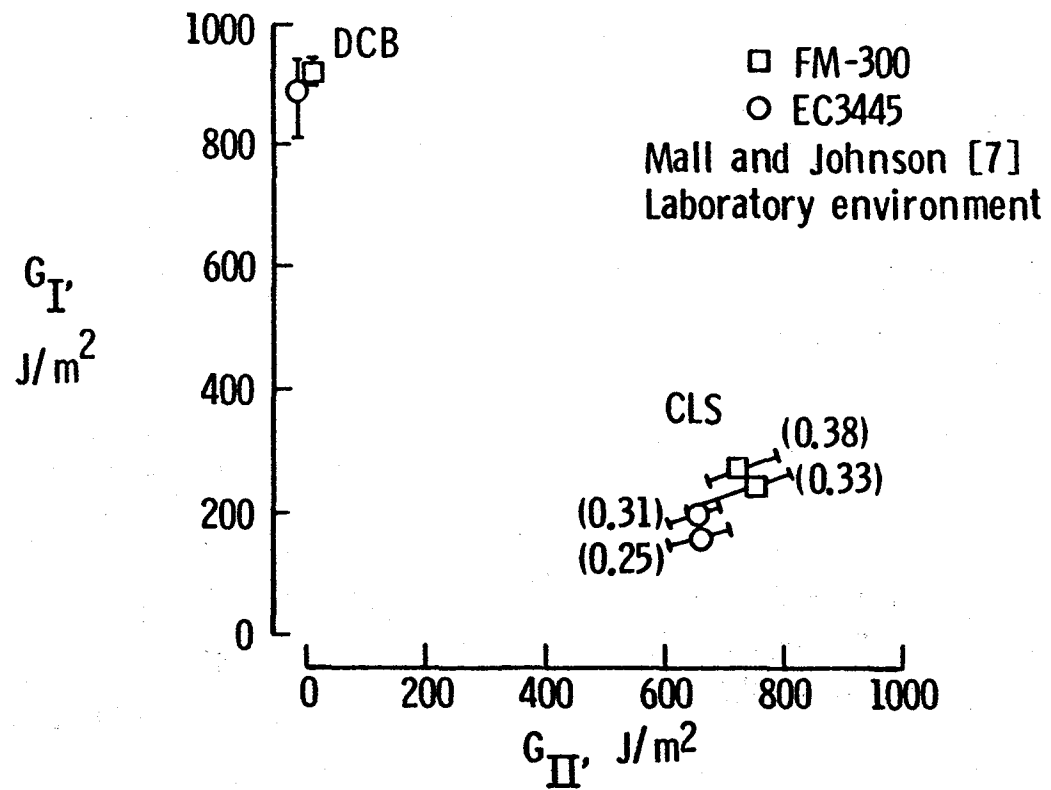


Figure 6 - Fracture toughness of FM-300 and EC 3445 adhesives; data spread is the maximum and minimum values.

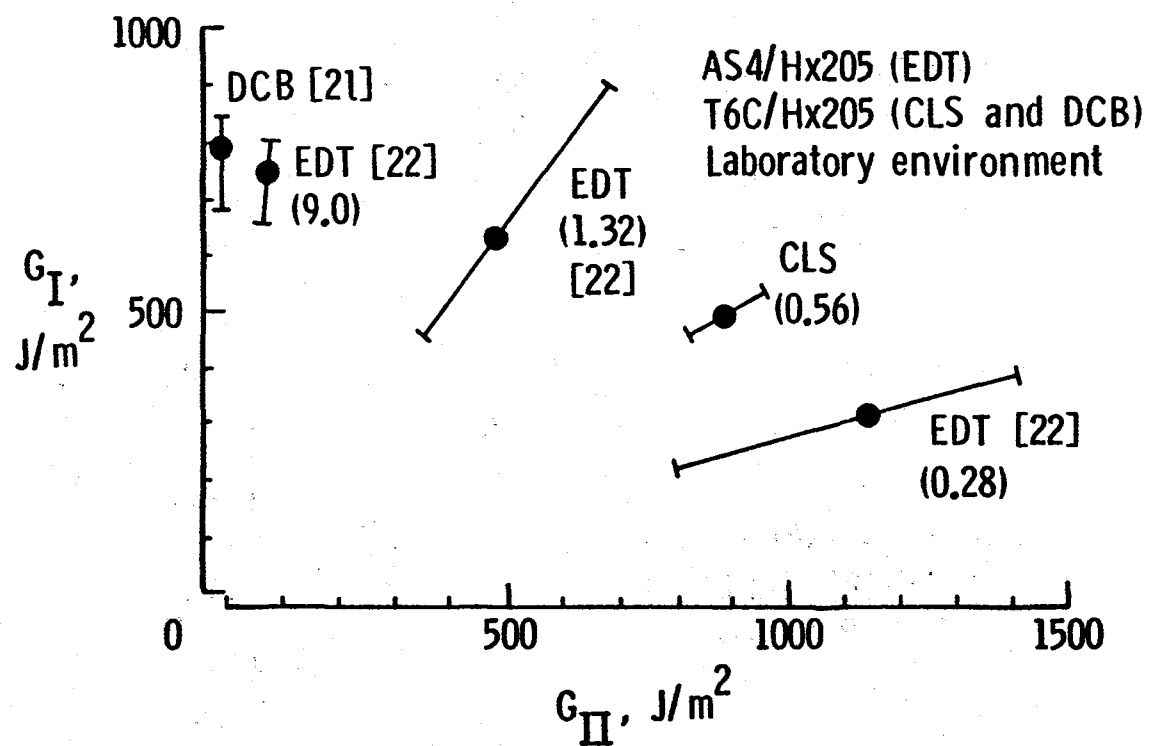


Figure 7 - Interlaminar fracture toughness of Hx205 matrix composites. The data spread is the maximum and minimum values.

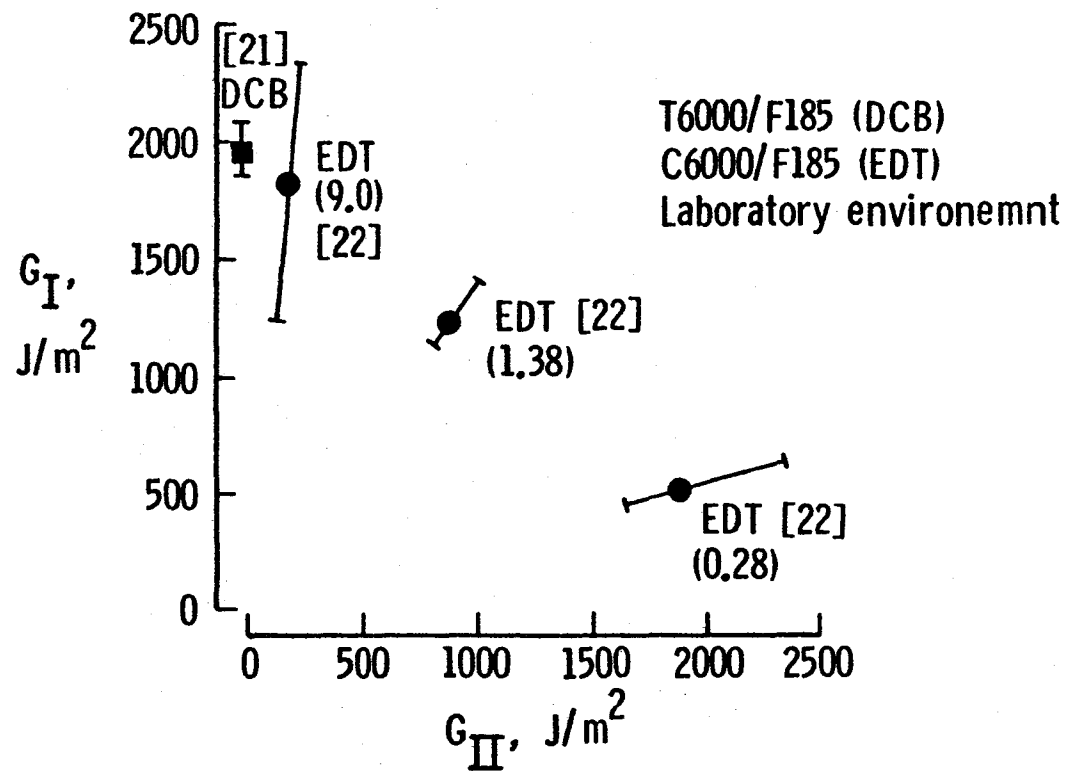


Figure 8 - Interlaminar fracture toughness of F185 matrix composites. The data spread is the maximum and minimum values.

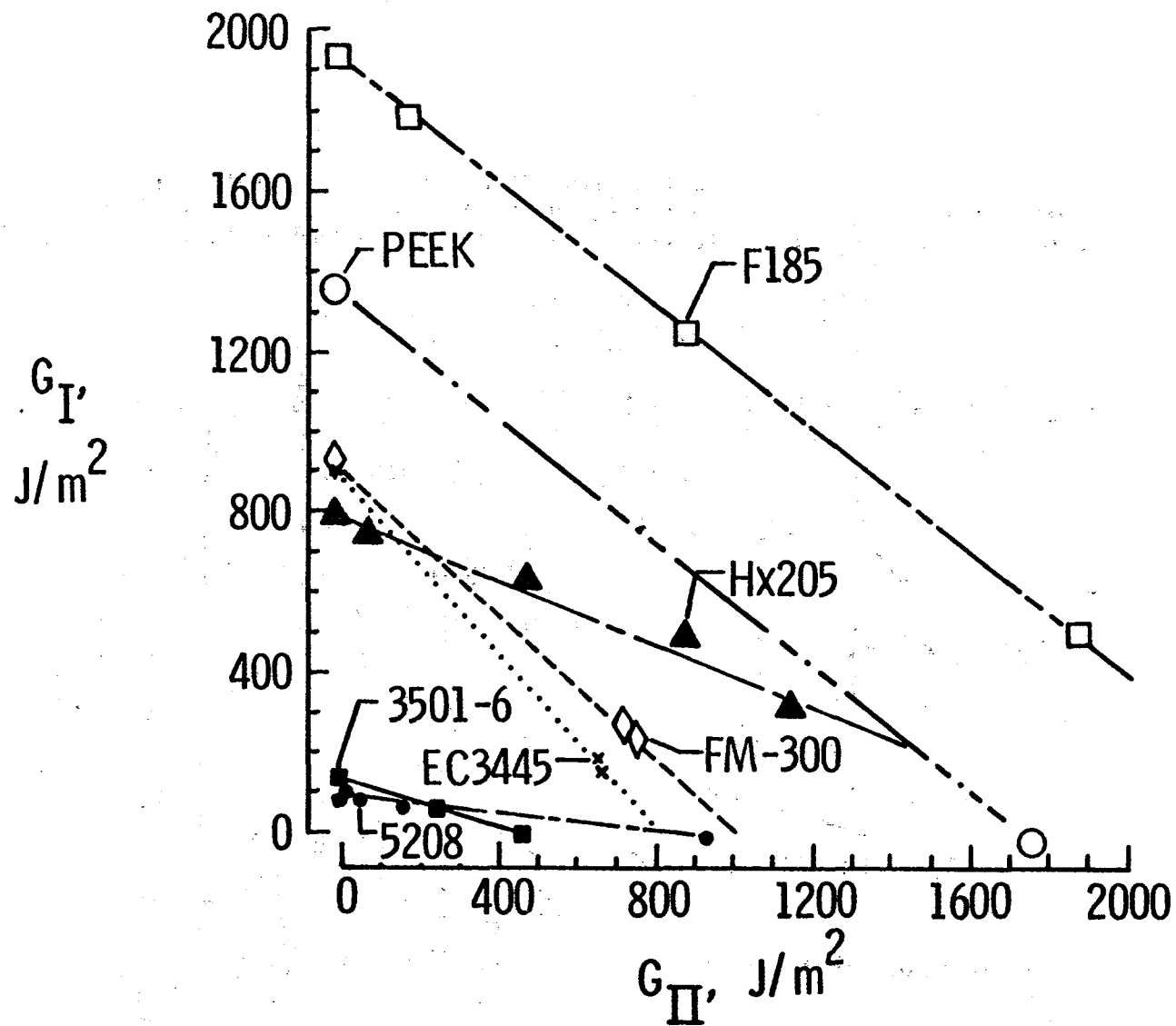


Figure 9 - Mixed mode fracture toughness.

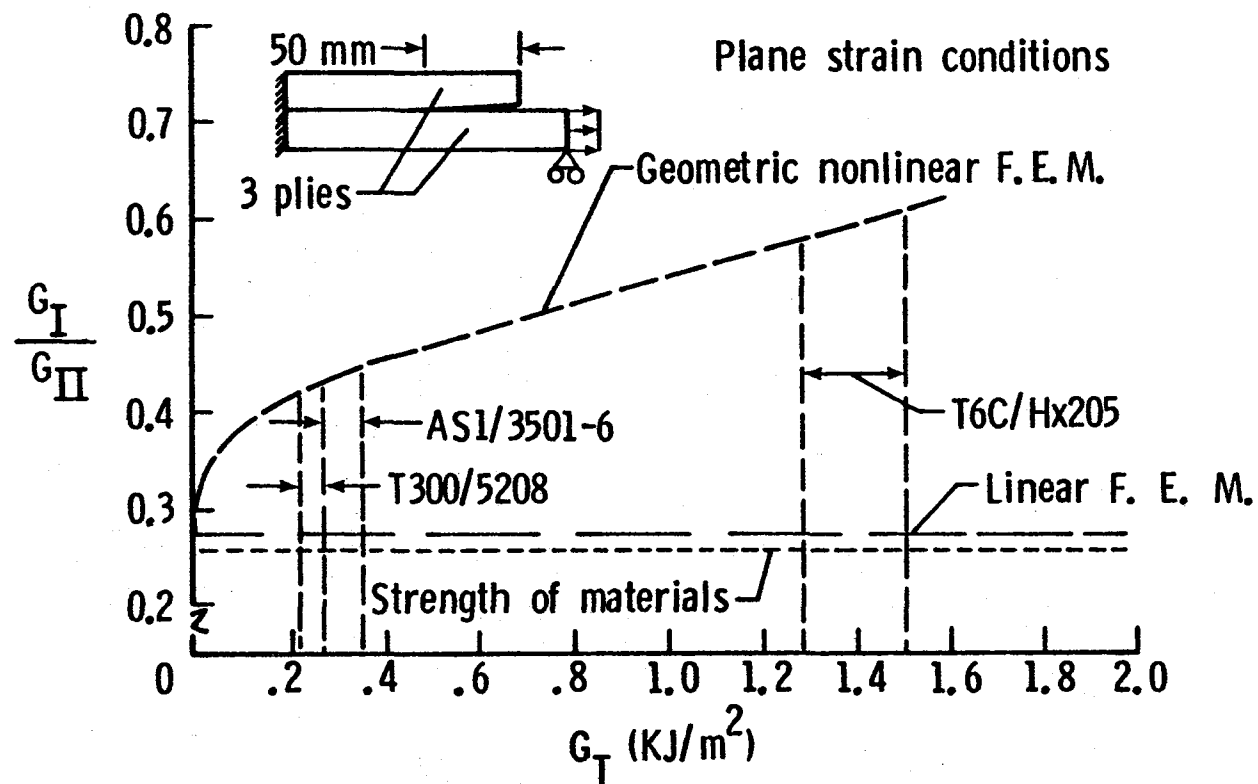


Figure 10 - Comparison of geometric linear and non-linear analysis to the strength of materials approach for calculating  $G_I/G_{II}$  ratio as a function of total strain-release rate of the delamination front.

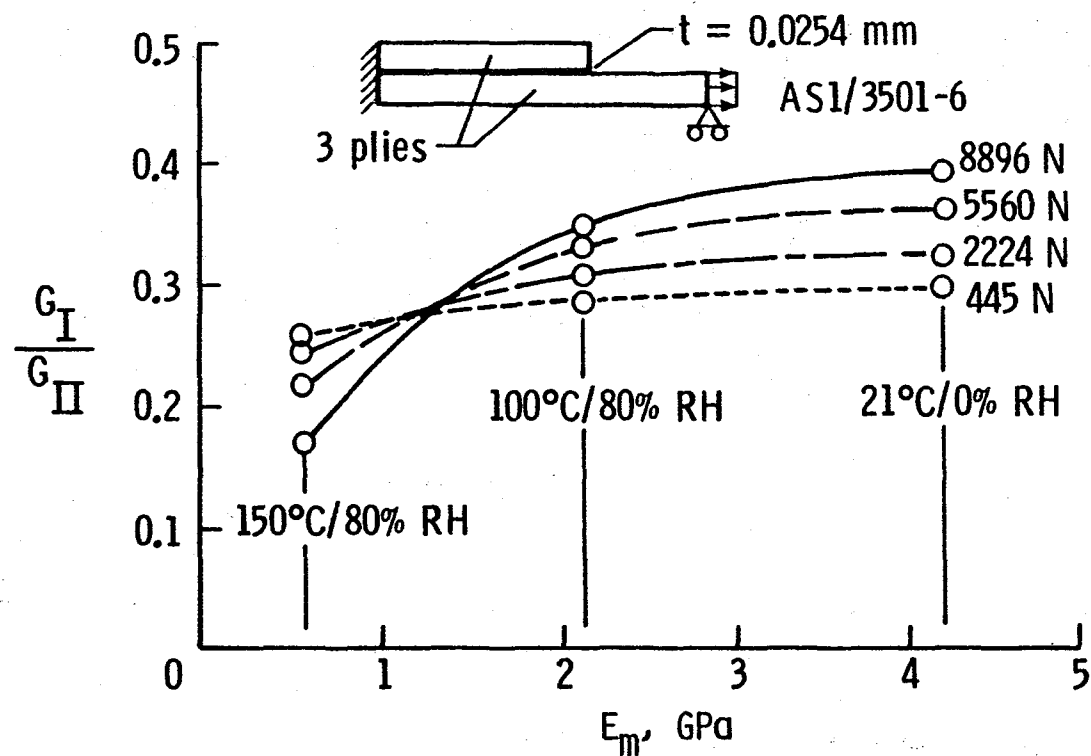


Figure 11 -  $G_I/G_{II}$  ratios as a function of applied load and matrix modules. The adherend properties were held constant.

1. Report No. NASA TM-87571		2. Government Accession No.		3. Recipient's Catalog No.	
4. Title and Subtitle Influence of the Resin on Interlaminar Mixed-Mode Fracture				5. Report Date July 1985	
				6. Performing Organization Code 505-33-33	
7. Author(s) W. S. Johnson P. D. Mangalgiri*				8. Performing Organization Report No.	
9. Performing Organization Name and Address NASA Langley Research Center, Hampton, VA 23665				10. Work Unit No.	
				11. Contract or Grant No.	
12. Sponsoring Agency Name and Address National Aeronautics and Space Administration Washington, DC 20546				13. Type of Report and Period Covered Technical Memorandum	
				14. Sponsoring Agency Code	
15. Supplementary Notes *P. D. Mangalgiri, NRC Resident Research Associate To appear as an ASTM Special Technical Publication of the same name.					
16. Abstract  Both literature review data and new data on toughness behavior of seven matrix and adhesive systems in four types of tests were studied in order to assess the influence of the resin on interlaminar fracture. Mixed mode (i.e. various combinations of opening mode I, $G_I$ , and shearing mode II, $G_{II}$ ) fracture toughness data showed that the mixed mode relationship for failure appears to be linear in terms of $G_I$ and $G_{II}$ . The study further indicates that fracture of brittle resins is controlled by the $G_I$ component, and that fracture of many tough resins is controlled by total strain-energy release rate, $G_T$ . Regarding the relation of polymer structure and the mixed mode fracture: high mode I toughness requires resin dilatation; dilatation is low in unmodified epoxies at room temperature/dry conditions; dilatation is higher in plasticized epoxies, heated epoxies, and in modified epoxies; modification improves mode II toughness only slightly compared with mode I improvements. Analytical aspects of the cracked lap shear test specimen were explored. Geometric nonlinearity must be addressed in calculating the $G_I/G_{II}$ ratio. The ratio varies with matrix modulus, which in turn varies with moisture and temperature.					
17. Key Words (Suggested by Author(s)) Interlaminar fracture toughness Adhesives Double cantilever beam specimen Edge delamination tension specimen Cracked lap shear specimen				18. Distribution Statement  Unclassified - Unlimited  Subject Category 24	
19. Security Classif. (of this report) Unclassified		20. Security Classif. (of this page) Unclassified		21. No. of Pages 38	
				22. Price A03	







3 1176 01316 1857